Nuclear Import of HSV-1 DNA Polymerase Processivity Factor UL42 Is Mediated by a C-Terminally Located Bipartite Nuclear Localization Signal[†]

Gualtiero Alvisi,*[,‡] Simone Avanzi,[‡] Daniele Musiani,[‡] Daria Camozzi,[‡,§] Valerio Leoni,[‡] Jennifer D. Ly-Huynh,[||] and Alessandro Ripalti[⊥]

Dipartimento di Ematologia e Scienze Oncologiche "L.A. Seragnoli", Università degli Studi di Bologna, Bologna, Italia, Department of Biochemistry and Molecular Biology, Monash University, Clayton, Victoria, Australia and ARC Centre of Excellence in Biotechnology and Development, and Azienda Ospedaliera Universitaria di Bologna Policlinico S. Orsola-Malpighi, Dipartimento di Patologia Clinica, Microbiologia, e Medicina Trasfusionale - Unità Operativa di Microbiologia, Bologna, Italia

Received May 12, 2008; Revised Manuscript Received October 18, 2008

ABSTRACT: The polymerase accessory protein of the human herpes simplex virus type 1 (HSV-1) DNA polymerase UL42 plays an essential role in viral replication, conferring processivity to the catalytic subunit UL30. We show here that UL42 is imported to the nucleus of living cells in a Ran- and energy-dependent fashion, through a process that requires a C-terminally located bipartite nuclear localization signal (UL42-NLSbip; PTTKRGRSGGEDARADALKKPK^{413}). Moreover cytoplasmic mutant derivatives of UL42 lacking UL42-NLSbip are partially relocalized into the cell nucleus upon HSV-1 infection or coexpression with UL30, implying that the HSV-1 DNA polymerase holoenzyme can assemble in the cytoplasm before nuclear translocation occurs, thus explaining why the UL42 C-terminal domain is not strictly required for viral replication in cultured cells. However, mutation of both UL30 and UL42 NLS results in retention of the DNA polymerase holoenzyme in the cytoplasm, suggesting that simultaneous inhibition of both NLSs could represent a viable strategy to hinder HSV-1 replication. Intriguingly, UL42-NLSbip is composed of two stretches of basic amino acids matching the consensus for classical monopartite NLSs (NLSA, PTTKRGR^{397}; NLSB, KKPK^{413}), neither of which are capable of targeting GFP to the nucleus on their own, consistent with the hypothesis that P and G residues in position +3 of monopartite NLSs are not compatible with nuclear transport in the absence of additional basic sequences located in close proximity. Our results showing that substitution of G or P of the NLS with an A residue partially confers NLS function will help to redefine the consensus for monopartite NLSs.

Human herpes simplex virus type 1 (HSV-1),[1] the principal alpha herpesvirus of humans, establishes latent infections and reactivates to cause recurrent infections causing a wide variety of clinical syndromes in newborns, children, and adults (*1*). Replication of its 153 kbp double-stranded DNA genome occurs in the nucleus of infected cells and requires a set of seven viral-encoded proteins (*2*), including a DNA polymerase, composed of a catalytic subunit, UL30, and a polymerase accessory protein (PAP), UL42, conferring processivity to the holoenzyme through a still unresolved mechanism (*3*−*8*). UL42 is a 488 amino acid, 65 kDa phosphoprotein that can be purified from infected cells together with the 1235 amino acid phosphoprotein UL30 (*9*). Interaction of UL30 with UL42 is crucial for the HSV-1 life cycle in that small molecules interfering with such an interaction also impair viral replication (*10*). The N-terminal two-thirds of the protein are sufficient to perform all known biochemical properties as a processivity factor, including the ability to bind dsDNA and UL30, as well as stimulate the activity of the latter (*11*−*13*). On the other hand, the C-terminal domain (CTD) of UL42 is not strictly required for viral replication in cultured cells, and its role in the context of viral infection is unknown (*14*). Consistent with its crucial role in HSV-1 DNA replication, UL42 is detectable within the nucleus of infected cells within 3 h after infection (*15*). Recent studies identified nuclear localization signals (NLSs) within the CTD of PAPs from several herpesviruses, including murine and human cytomegalovirus (CMV) and

[†] This work was partly supported by the University of Bologna and the Italian Ministry of Education (60% and 40%) and the AIDS Project of the Italian Ministry of Public Health.

* Corresponding author. Tel: +39(0)514290919. Fax: +39(0)51307397. E-mail: gualtiero.alvisi3@unibo.it.

[‡] Università degli Studi di Bologna.

[§] Present address: Laboratory of Cell Biology, Istituto Ortopedico Rizzoli, Bologna, Italia

[||] Monash University and ARC Centre of Excellence in Biotechnology and Development.

[⊥] Azienda Ospedaliera Universitaria di Bologna Policlinico S. Orsola-Malpighi.

[1] Abbreviations: HSV-1, herpes simplex virus type 1; NLS, nuclear localization signal; NLShyd, hydrophobic NLS; NLSbip, bipartite NLS; UL42-BD, UL42 binding domain; CMV, cytomegalovirus; HHV, human herpesvirus; CTD, C-terminal domain; NPC, nuclear pore complex; IMP, importin; IBB domain, importin beta binding domain; trIMPα, IBB truncated IMPα; GFP, green fluorescent protein; DMEM, Dulbecco's modified Eagle's medium; DAPI, 4′,6-diamidino-2-phenylindole; PAGE, polyacrylamide gel electrophoresis; mAb, monoclonal antibody; NTF2, nuclear transport factor 2; ORF, open reading frame; PBS, phosphate-buffered saline; PMSF, phenylmethanesulfonyl fluoride; PVDF, polyvinylidene difluoride; TBS, Tris-buffered saline; TRITC, tetramethyl rhodamine isothiocyanate; Hepes, *N*-2-hydroxyethylpiperazine-*N*′-2-ethanesulfonic acid; SDS, sodium dodecyl sulfate.

10.1021/bi800869y CCC: $40.75
Published on Web 12/03/2008

human herpesviruses 7 and 8 (HHV-7 and -8) strongly suggesting an important role in viral replication for this domain (*16*−*19*). Because nuclear targeting of herpesviral DNA polymerases is a key event for viral replication, those NLSs have been proposed as potential therapeutic targets (*16, 17, 20, 21*).

The eukaryotic cell nucleus is separated from the rest of the cell by a double membrane structure, the nuclear envelope, the only passage through which is provided by the multiprotein-constituted nuclear pore complexes (NPCs). Molecules larger than 60−90 kDa need to be actively translocated into the nucleus in an NLS-dependent fashion through the action of members of the importin (IMP) superfamily of intracellular transporters, which mediate docking of the NLS-containing protein to the NPC and translocation through it into the nucleus (*22*). A well-characterized class of NLS is recognized by the IMPα/*β* heterodimer, where IMPα recognizes the NLS, and IMP*β* facilitates the IMP−NLS interaction by directly binding to an autoinhibitory domain in IMPα, the IMP*β* binding (IBB) domain, thus increasing the affinity of the IMPα−NLS interaction (*23*). Once translocation through the NPC is complete, binding of Ran complexed with GTP to IMP*β* results in the dissociation of IMP*β* from the IMPα−NLS complex (*24*), releasing the IBB autoinhibitory domain, thus promoting the dissociation between IMPα and the cargo protein within the nucleus. Ran is a small GTPase protein, which is mainly found in its GDP-bound form in the cytoplasm, whereas it is almost exclusively bound to GTP in the nucleus, thus ensuring the directionality of nuclear transport processes (*25*).

In mammalian cells, six different isoforms of IMPα have been identified, which fall in three phylogenetically distinct groups, the α-S, α-P, and α-Q, differing for cargo specificity and exhibiting unique temporal and spatial expression patterns (*26, 27*). IMPα-recognized NLSs comprise both monopartite NLSs, single clusters of basic residues, similar to that characterized extensively for the simian virus SV40 large tumor antigen, and bipartite NLSs formed by two closely located basic clusters, reminiscent of that originally described for the *Xenopus laevis* histone chaperone nucleoplasmin (*28*). Based on structural and thermodynamic data (*29, 30*), the consensus sequence for classical monopartite NLSs has been defined as K-(K/R)-X-(K/R), with X being any amino acid. However, recent findings from our group demonstrated that a P residue in position +3 of the NLS core is not compatible with NLS function, suggesting K-(K/R)-X′-(K/R), with X′ being any amino acid except P, as a new, more appropriate consensus (*20*).

In HHV-8, the C-terminally located NLS of the PAP, PF-8, is believed to be responsible for nuclear targeting of the DNA polymerase holoenzyme, in that PF-8 is able to relocalize to the cell nucleus the otherwise cytoplasmic catalytic subunit (*17*). The HCMV PAP ppUL44 also contains a functional NLS, whose activity is important for nuclear targeting of other viral proteins, including the DNA polymerase catalytic subunit pUL54 and the uracil DNA glycosilase, ppUL114 (*16, 21, 31*). In the case of HSV-1, two functional NLSs have already been identified on the catalytic subunit of the DNA polymerase UL30: one of them is a noncanonical NLS, containing crucial hydrophobic residues (NLShyd: RRMLHR^{1229}) and is located at the C-terminus of the protein within the binding domain for UL42 (residues 1209−1235) (*32, 33*). On the other hand, a classical bipartite NLS (NLSbip: PAKRPRETPSPADPPG-GASKPRK^{1136}) is located upstream of the UL42 binding domain (UL42-BD) and is believed to play a major role in determining UL30 nuclear localization (*20*). Intriguingly, UL42 CTD possesses two putative basic NLSs, which are closely located and could potentially form a bipartite NLS. Hence, although UL42 CTD has been shown not to be absolutely required for viral replication (*14*), it might play an important role in HSV-1 infection.

The aim of this study was to address the importance of UL42 CTD in UL42 nuclear import and to investigate whether HSV-1 DNA polymerase holoenzyme can be imported to the nucleus as a complex, in a similar fashion to that reported for HHV-8 and HCMV (*17, 21*). Here we report the characterization of the UL42 nuclear import pathway, identifying a bipartite NLS (NLSbip, PTT-KRGRSGGEDARADALKKPK^{413}) encompassing two putative monopartite NLSs (NLSA and NLSB), which is necessary for UL42 active nuclear transport. We also show that nuclear translocation of UL42 is similar to that of other herpesvirus homologues in terms of sensitivity to a Ran dominant negative mutant, energy requirement, and IMP involvement, implying a classical nuclear import pathway. Finally we show that mutant derivatives of UL30 and UL42 impaired for nuclear targeting can be efficiently imported into the nucleus when expressed with the wild-type form of the other subunit, suggesting that the HSV-1 DNA polymerase holoenzyme can be imported into the nucleus as a complex and explaining why NLS mutant derivatives of UL42 can be targeted to nuclear replication compartments (RC) upon viral infection. Importantly mutation of both UL30 and UL42 NLSs resulted in retention of the DNA polymerase holenzyme in the cytoplasm, strongly suggesting that both UL42 and UL30 NLSs could represent viable therapeutic targets to hinder HSV-1 replication.

MATERIALS AND METHODS

Construction of Expression Plasmids. UL42 fusion protein expressing vectors were generated using the Gateway system (Invitrogen). Primers including the attB1 and attB2 recombination sites were used to amplify the UL42 sequences of interest, with plasmid pBE5.1 as a template (*6*). Polymerase chain reaction fragments were introduced into plasmid vector pDONOR207 (Invitrogen) via the BP recombination reaction, according to the manufacturer's recommendations to generate the entry clones pDNR-UL42(2−488), pDNR-UL42(2−413), pDNR-UL42(2−397), pDNR-UL42(2−390), pDNR-UL42(391−488), pDNR-UL42(391−413). pDNR-UL42(391−488)-NLSAm, pDNR-UL42(391−488)-NLSBm, and pDNR-UL42(391−488)-NLSABm, carrying point mutations within UL42-NLSA (wdpGRSGGEDARADTAL-KKPK^{413}), UL42-NLSB (PTTKRGRSGGEDARADrg-LlePK^{413}), or both NLSs, respectively, were generated using the Quickchange mutagenesis kit (Stratagene) and appropriate oligo pairs, according to the manufacturer's recommendations, using vector pDNR-UL42(391−488) as a template. The mutagenic primers were designed to insert a *Bam*HI restriction site within NLSA and an *Xho*I site within NLSB. To generate full-length UL42-NLSs point mutants, we first

created the pDNR-UL42(2−397)-NLSAm construct, containing a *Bam*HI site within the mutagenized NLSA (PTrdpGRS^{397}), followed by a *Hin*dIII restriction site, using plasmid pDNR-UL42(2−488) as a template. The *Bam*HI−*Hin*dIII fragment obtained by enzymatic restriction of plasmid pDNR-UL42(391−488)-NLSAm, was then cloned into plasmid pDNR-UL42(2−397)-NLSAm to generate plasmid pDNR-UL42(2−488)-NLSAm, containing the point mutation PTrdpGRSGGEDARADTALKKPK^{413}. We also created pDNR-UL42(2−413)-NLSBm (PTTKRGRSGGEDARADTALlePK^{413}), containing a *Xho*I restriction site within mutagenized NLSB, using plasmid pDNR-UL42(2−488) as a template and an appropriate oligo pair. The *Xho*I−*Hin*dIII fragment obtained by enzymatic restriction of plasmid pDNR-UL42(391−488)-NLSBm was then cloned into plasmid pDNR-UL42(2−413)-NLSBm to generate plasmid pDNR-UL42(2−488)-NLSBm, containing the point mutation (PTTKRGRSGGEDARADTALlePK^{413}) within UL42-NLSB. We also generated plasmid pDNR-UL42(2−413)-NLSABm (PTrdpGRSGGEDARADTALlePKT^{413}), containing an *Xho*I site within mutagenized NLSB, by using plasmid pDNR-UL42(2−488)-NLSAm as a template and an appropriate oligo pair. The *Xho*I−*Hin*dIII fragment obtained by enzymatic restriction of plasmid pDNR-UL42(391−488)-NLSBm was then cloned into plasmid pDNR-UL42(2−413)-NLSABm to generate plasmid pDNR-UL42(2−488)-NLSABm, containing point mutations within both UL42-NLSs (PTrdpGRSGGEDARADTALlePKT^{413}). Construct pDNR-UL42(391−488);G396A-NLSBm, carrying a G to A substitution in position +3 within the core of UL42-NLSA and point mutations within UL42-NLSB (PTTKRaRSGGEDARADrgLlePK^{413}), was generated using the Quickchange mutagenesis kit (Stratagene) and an appropriate oligo pair, according to the manufacturer's recommendations, using construct pDNR-UL42(391−488)-NLSBm as a template. Plasmids pDNR-UL42(391−397) and pDNR-UL42(391−397);G396A were generated using plasmid pDNR-UL42(2−488) as a template and an appropriate oligo pair. These constructs, in turn, were used to perform LR recombination reactions with the Gateway system compatible expression plasmids pEPI-DEST-GFP (*34*), pBkCMV-DsRed2 (*35*), or pDEST-FLAG (*36*), in order to generate mammalian expression vectors encoding differently tagged fusion proteins (see Figure 2A).

Primers including the attB1 and attB2 recombination sites were used to amplify the mouse IMPα2 and IMPα4 coding sequences lacking the IBB autoinhibitory domain, using plasmids pGEX6P2-GFP-mRch1 and pGEX6P2-GFP-Qip as templates, respectively (*37*). Polymerase chain reaction fragments were introduced into plasmid vector pDONOR207 (Invitrogen) via BP recombination reactions to generate the entry clones pDNR-IMPα2(70−530) and pDNR-IMPα4(95−522). These constructs, in turn, were used to perform LR recombination reactions with the Gateway system compatible expression plasmid pEPI-DEST-GFP (*34*), in order to generate mammalian expression vectors pEPIGFP-trIMPα2 and pEPIGFP-trIMPα4, encoding GFP-tagged mouse IMPαs lacking the autoinhibitory IBB domain. Plasmids pEPIGFP-UL30(2−1235), pEPIGFP-UL30(2−1235)-NLS2m, pEPIGFP-UL30(1114−1136), pEPIGFP-UL44(2−433), pEPIGFP-UL44(2−433)ΔNLS, pBkDsRed2-UL44(2−433), and pBkDsRed2-UL44(2−433)ΔNLS encoding fusion proteins between spontaneously fluorescent proteins and the HSV-1 DNA polymerase catalytic subunit UL30 or the HCMV processivity factor ppUL44 have been described (*20*, *38*). Plasmid DsRed−RanQ69L, encoding a dominant negative form of Ran unable to hydrolyze GTP and bind to NTF2, thus impairing active nuclear transport (*39*), was kindly provided by Michel Green (University of Massachusetts). Plasmid pBE5.1, containing the UL42 ORF from HSV-1 (*6*) was a generous gift from Charles Hwang (State University of New York Upstate Medical University). Plasmid pEGFP-N1-H1E (*40*), enabling the expression of a fusion protein between GFP and histone H1E was provided by Gabi Gerlitz (NIH). The Gateway technology compatible vector pDEST-FLAG (*36*) was provided by Emanuele Panza (University of Bologna). Plamids pGEX6P2-GFP-mRch1, pGEX6P2-GFP-Qip, and pEGFP-C1-trIMPα6 (*37*), encoding a fusion protein between GFP and mouse IMPα6 lacking the autoinhibitory IBB domain (residues 101−534) were generous gifts from Yoichi Miyamoto (Monash University). The integrity of all constructs was confirmed by DNA sequencing (Primm).

Cell Culture and Transfection. COS-7, Vero, and HEK 293 cells were maintained in Dulbecco's modified Eagle's medium (DMEM) supplemented with 5% (v/v) fetal bovine serum, 50 U/mL penicillin, 50 U/mL streptomycin, and 2 mM L-glutamine. For live cell imaging experiments, cells were trypsinized and seeded onto 2 mm glass-bottom WillCo dishes (WillCo wells) 1 day before transfection, which was performed using Lipofectamine 2000 (Invitrogen), according to the manufacturer's specifications. For transfection/infection experiments, Vero cells were trypsinized and seeded onto glass coverslips 1 day before transfection, which was performed as above. Thirty hours after transfection, cells were infected with a HSV-1 clinical isolate at a multiplicity of infection (MOI) of 5 for 1 h at 37 °C. Seven hours after infection, cells were fixed in methanol/acetone 3:1 for 20 min at −20 °C. For Western blot and coimmunoprecipitation experiments, cells were trypsinized and seeded onto six well multiwell plates or onto 10 cm dishes, respectively, 1 day before transfection.

Fluorescence Microscopy and Image Analysis. Live COS-7 and Vero cells, grown on WillCo dishes (WillCo wells) and expressing GFP and DsRed fusion proteins, were imaged using a Nikon Eclipse TE2000-U inverted microscope (Nikon) equipped with a Nikon DXN1200 digital camera and a Nikon Plan Fluor 40× objective (Nikon). Digital images were obtained using the NIS elements software (Nikon), using the following settings: gain, 50; offset, 0; acquisition times 500−2000 ms. Semiquantitative analysis of the levels of nuclear accumulation relative to each GFP-fusion protein was performed using the ImageJ 1.62 public domain software (NIH) to perform single cell measurements of the nuclear (F_n) and cytoplasmic (F_c) fluorescence, subsequent to the subtraction of fluorescence due to autofluorescence/background, to determine the nuclear to cytoplasmic fluorescence ratio (F_n/F_c). Localization of each cell was classified on the basis of the F_n/F_c ratio as exclusively nuclear (N; $F_n/F_c > 10$), mainly nuclear (N > C; $10 > F_n/F_c > 2$), diffuse (D; $2 > F_n/F_c > 1$) or mainly cytoplasmic (C > N; $F_n/F_c < 1$). At least 100 GFP expressing cells were analyzed for each fusion protein. Each experiment has been repeated three times.

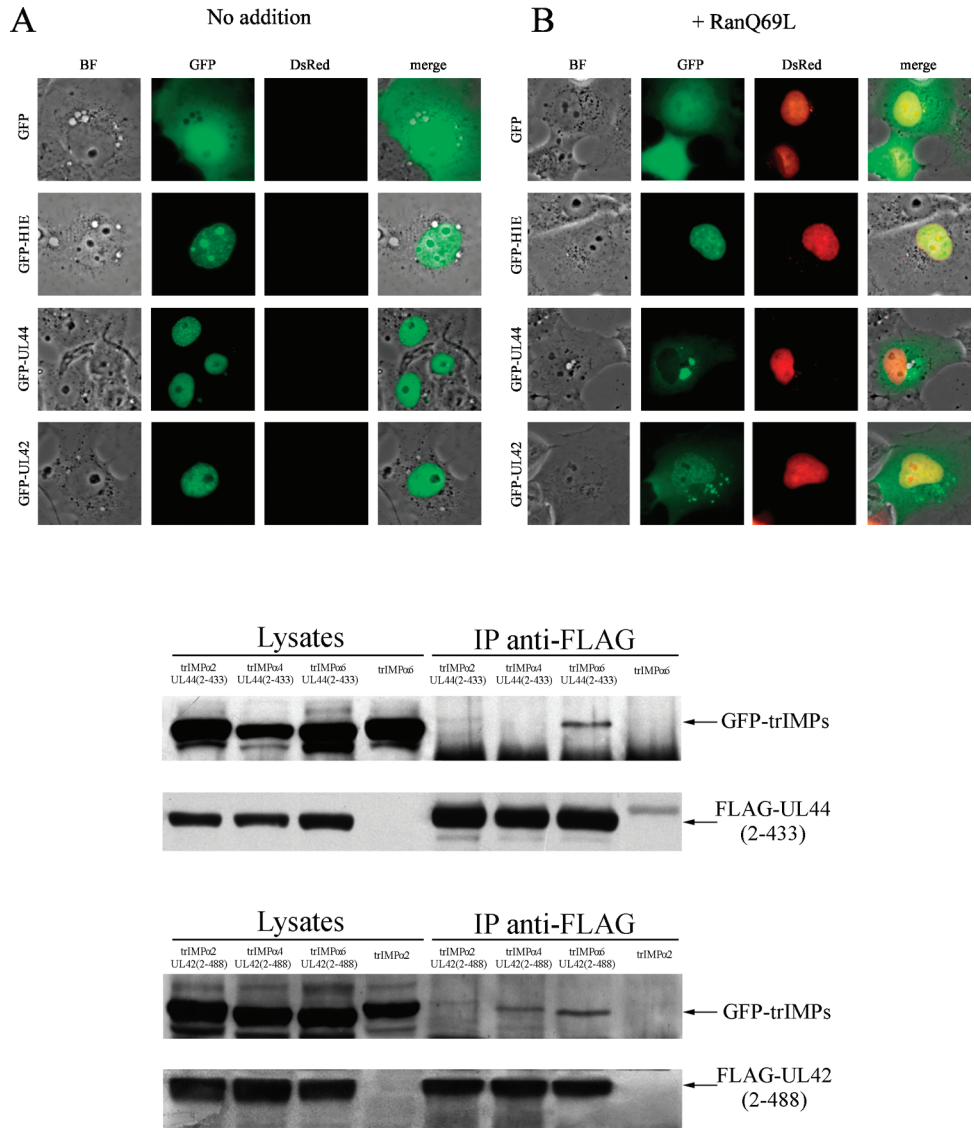

FIGURE 1: HSV-1 DNA polymerase processivity factor UL42 interacts with IMPα and its nuclear import is inhibited by RanQ69L. Fluorescent images of live COS-7 cells 16−24 h after transfection to express the indicated GFP fusion proteins in the absence (A) or presence (B) of DsRed−RanQ69L. The bright field (BF), green (GFP), and red (DsRed) channels are shown, and a merged image is shown in the right panels. (C) HEK 293 cells were transfected to express the indicated fusion proteins. Cells were harvested 24 h after transfection and immunoprecipitated using the anti-FLAG mAb, as described in Materials and Methods. After SDS−PAGE separation and transfer to nitrocellulose, purified proteins were detected using anti-GFP (top lanes) or anti-FLAG mAbs (bottom lanes). The presence of immunoprecipitated fusion proteins is indicated by arrows.

For indirect immunofluorescence assays (IIFA), cells grown on coverlips and fixed in methanol/acetone were incubated with the gD specific mouse monoclonal antibody (mAb) HD1 (1:400, a generous gift from Gabriella Campadelli-Fiume, University of Bologna), followed by incubation with a TRITC coupled secondary antibody (Cappel; 1:100). DNA was stained with 4′,6-diamidino-2-phenylindole (DAPI; 300 nM) for 5 min. Coverslips were mounted with PBS/glycerol on glass slides and analyzed using a Nikon Eclipse E600 microscope (Nikon), equipped with a Nikon DXN1200 digital camera and a Nikon Plan Fluor 100× oil immersion objective (Nikon).

Western Blot Analysis. For the analysis of GFP−UL42 fusion protein expression levels, cells grown on six well multiwell plates were harvested in 100 μL of RIPA buffer (50 mM Tris-cl, pH 7.4; 150 mM NaCl; 1% NP40; 0.25% sodium deoxycholate; 1 mM PMSF) 48 h after transfection. Ten microliters of the cell lysates was loaded onto 10% bistrisacrylamide gels and separated by polyacrylamide gel electrophoresis (PAGE). Electrophoretically separated proteins were then transferred to a PVDF membrane (Amersham), which was blocked in buffer A [5% bovine serum albumin (BSA) (w/v) and TBS 1×] for 1 h at room temperature and washed 3 times with buffer B (0.05% Tween and TBS 1×). Detection of fusion proteins was performed by incubating the membranes with anti-GFP mouse mAb sc-9996 (SantaCruz Biotechnologies; 1:400) and a peroxidase coupled secondary antibody (SIGMA; 1:400). The immunoblots were developed with the horseradish peroxidase substrate 4-Cl-1-naphtol (Biorad) in the presence of H_2O_2.

Energy Depletion Assays. Intracellular ATP was depleted by incubating cells for 30 min at 37 °C in DMEM containing no glucose, 5% fetal bovine serum, and supplemented with 10 mmol/L sodium azide and 6 mmol/L 2-deoxy-D-glucose (Sigma). After this treatment, the ATP intracellular levels were restored by replacing the energy depletion medium with

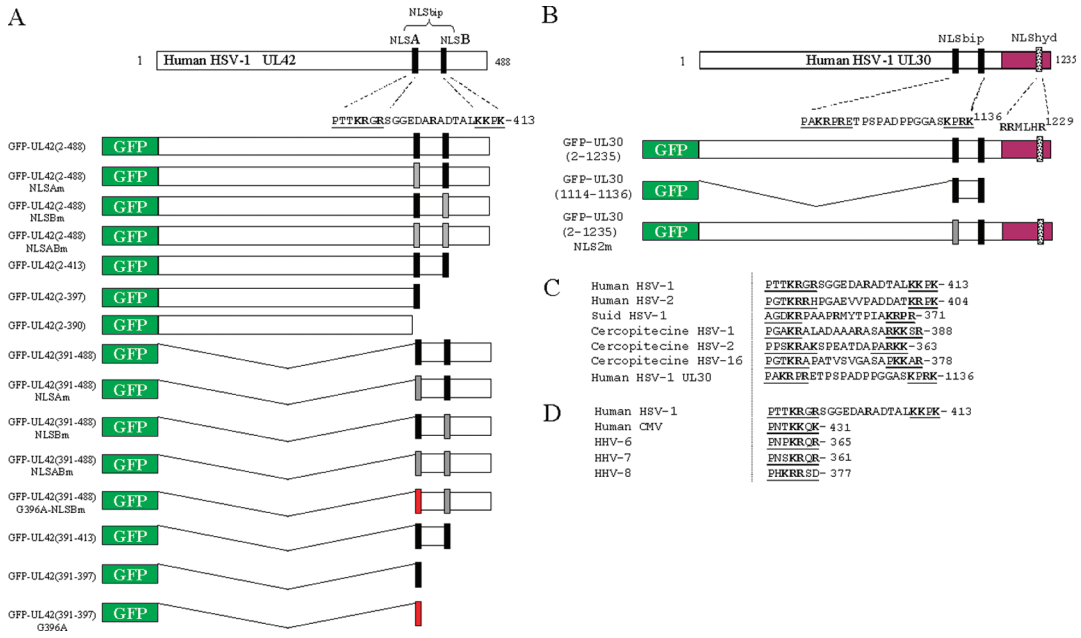

FIGURE 2: UL42 contains two putative basic NLSs located at the C-terminus, which are conserved among α-herpesviruses. (A) Schematic representation of the HSV-1 UL42 DNA polymerase processivity factor coding sequence, of its putative bipartite NLS, and of the GFP−UL42 mutant derivatives expressed in this study. Basic monopartite NLSs, black bars; NLSs containing point mutations, gray bars; UL42-NLSA containing a G396A substitution, red bar; the single letter amino acid code is used; basic residues are in bold; putative monopartite NLSs are underlined. (B) Schematic representation of the HSV-1 UL30 DNA polymerase catalytic subunit coding sequence, of its NLSs, of the UL42 binding site, and of the GFP−UL30 mutant derivatives expressed in this study. Basic arms of UL30 bipartite NLSs, black bars; noncanonical hydrophobic NLS, dotted bars; UL42-BD, purple boxes; NLSs containing point mutations, gray bars; the single letter amino acid code is used. (C) Comparison of human HSV-1 UL42 bipartite NLS coding sequence to that of homologues from other α-herpesviruses and to HSV-1 UL30 DNA catalytic subunit; the single letter amino acid code is used; basic residues are in bold; putative monopartite NLSs are underlined. (D) Comparison of human HSV-1 UL42 bipartite NLS coding sequence to that of homologues from other herpesviruses; the single letter amino acid code is used; bold indicates basic residues; putative monopartite NLSs are underlined.

DMEM, as used in normal growing conditions. Each experiment has been repeated three times.

Immunoprecipitation of FLAG Fusion Proteins. Twenty-four hours post-transfection, HEK 293 cells were harvested and washed with PBS. Cells were lysed in lysis buffer [50 mM Hepes (pH 7.4), 100 mM NaCl, 1% Nonidet-P 40, Complete Mini EDTA-free Protease Inhibitor Cocktail Tablets (Roche Applied Science)] for 10 min on ice and sonicated at low intensity for 10 s. After clarification, supernatants were incubated with 4 μg of the anti-FLAG mAb (SIGMA) overnight at 4 °C, with gentle rocking. The following day, 30 μL of protein A/G beads (Santa Cruz Biotechnology) were added and incubated for 4 h. After washes with lysis buffer, beads were resuspended in 2× Laemmli's buffer, boiled at 95 °C and centrifuged at 16000 × *g* for 5 min before the supernatant was analyzed by 10% SDS−PAGE and Western blotting using the anti-GFP sc-9996 (SantaCruz Biotechnologies; 1:10000) and anti-FLAG (SIGMA; 1:5000) mAbs, followed by incubation with a peroxidase coupled secondary antibody (SIGMA; 1:10000). The immunoblots were developed with ECL plus (Amersham).

RESULTS

UL42 Is Actively Transported to the Nucleus of Mammalian Cells and Binds to IMPs in the Absence of Other Viral Proteins. Consistently with its pivotal role in HSV-1 DNA replication, UL42 strongly localizes within the cell nucleus both during viral infection and when expressed in the absence of other viral proteins (*14*). We decided to visualize UL42 subcellular localization within living cells by expressing a GFP−UL42 fusion protein. We transiently expressed GFP−UL42(2−488) in COS-7 cells and analyzed its subcellular localization by live imaging using an inverted microscope (Figure 1). We also expressed GFP alone, which lacks specific localization signals, GFP−UL44(2−433), which is transported to the nucleus by the IMPα/β heterodimer, and GFP−H1E, which is imported into the nucleus via multiple pathways and strongly binds to chromatin, as negative and positive controls for nuclear targeting (*16, 41*). As expected, GFP localized with a diffuse pattern within the cells, whereas both GFP−UL44(2−433) and GFP−H1E strongly accumulated in the nucleus, with GFP−UL44(2−433) showing its typical speckled pattern and GFP−H1E accumulating in the perinucleolar region, consistent with its ability to interact with chromatin (*41*). Importantly, GFP−UL42(2−488) also strongly localized in the nucleus of transfected cells, often resulting in the formation of nuclear speckles, reminiscent of those reported for its HCMV and HHV-7 homologues (*16, 19*), showing that tagging UL42 with GFP did not alter its nuclear localization properties.

UL42 is a 65 kDa protein and may be therefore able to enter into the nucleus by passive diffusion. However, its strong nuclear localization during both viral infection and ectopic expression (*14*) suggests that UL42 is actively transported into the cell nucleus. To verify this hypothesis, we analyzed the subcellular localization of GFP−UL42(2−488) in living cells in the presence of DsRed−RanQ69L, a Ran dominant negative mutant unable to hydrolyze GTP (*42*). Since binding of Ran−GTP to IMPβ determines the release

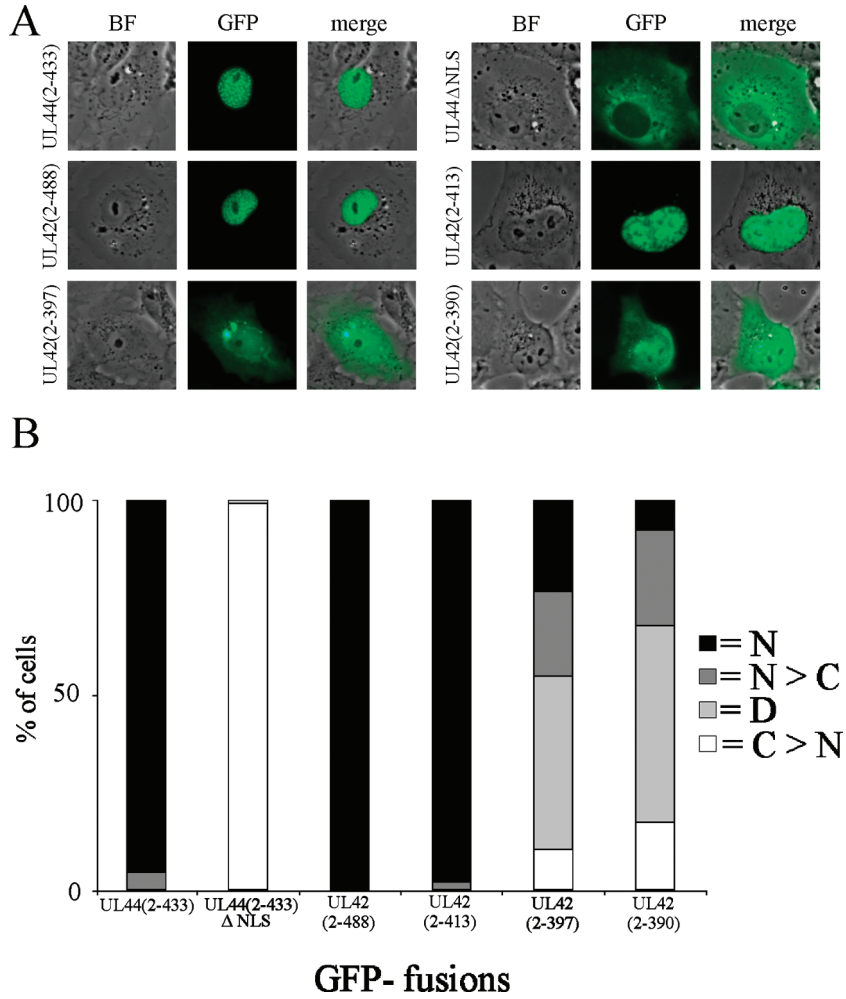

FIGURE 3: UL42 residues 391−488 are required for optimal nuclear targeting. (A) Fluorescent images of live COS-7 cells 16−24 h after transfection to express the indicated GFP fusion proteins. The bright field (BF) and the green (GFP) channels are shown, and a merged image (merge) is shown in the right panels. (B) GFP-expressing cells (n > 100) were scored on the basis of the GFP fusion subcellular localization. N = exclusively nuclear; N > C = more nuclear than cytoplasmic; D = diffuse; C > N = more cytoplasmic than nuclear (see Materials and Methods).

of the NLS-containing cargoes from IMPα, overexpression of RanQ69L impairs active nuclear transport by preventing the interaction of classical NLSs with IMPs (*39*). We also expressed GFP, GFP−UL44(2−433), and GFP−H1E as controls.

As expected, coexpression with RanQ69L did not affect GFP subcellular localization. Moreover, coexpression of RanQ69L with GFP−H1E did not significantly inhibit its nuclear localization, reflecting its ability to enter the nucleus by passive diffusion and then to strongly bind to cellular chromatin (Figure 1B). By contrast, upon coexpression with RanQ69L, GFP−UL44(2−433) was retained mainly in the cytoplasm, with a localization similar to that of GFP−UL44ΔNLS, a ppUL44 point mutant derivative containing the PNTKKQK^{431} to PNTvaQI^{431} substitutions inactivating its NLS (*16*) (see also Figure 3), consistent with its IMPα/β-dependent import pathway. When GFP−UL42(2−488) was expressed in the presence of RanQ69L, a significant amount of protein became detectable in the cytoplasm (Figure 1B), indicating that UL42 nuclear import is inhibited by RanQ69L and is therefore likely to be an IMP-mediated process. To verify this hypothesis, we transfected HEK293 cells to express the FLAG epitope versions of both UL44 and UL42 in the presence of truncated IMPαs (trIMPαs), lacking the autoinhibitory IBB domain and thus binding to NLSs with an affinity comparable to that of the IMPα/β heterodimer (*43, 44*). Since different IMPα isoforms have unique NLS binding specificity, we tested one member of each IMPα subgroup: IMPα2, IMPα4, and IMPα6, belonging to the IMPα-P, α-Q, and α-S subgroups, respectively. Proteins were immunoprecipitated using the FLAG antibody from cells expressing either the FLAG−UL44(2−433) or the FLAG−UL42(2−488) fusion proteins in the presence of the GFP−trIMPα2, GFP−trIMPα4, or GFP−trIMPα6 fusion proteins. As shown in Figure 1C, the FLAG−UL44(2−433) fusion protein could be coimmunoprecipitated with GFP−trIMPα6 and to a lesser extent with GFPtr-IMPα2. No specific signal could be detected for GFP−trIMPα4. On the other hand FLAG−UL42(2−488) could be efficiently immunoprecipitated with both GFP−trIMPα4 and GFP−trIMPα6 and, as in the case of ppUL44, only to a lesser extent with GFP−trIMPα2 (Figure 1C). No specific signal for GFP−trIMPαs could be detected after immunoprecipitation of lysates of cells transfected to express GFP−trIMPαs but not FLAG fusion proteins (see Figure 1C).

UL42 CTD Is Required for Optimal Nuclear Targeting. IMPs mediate active nuclear import of cargo proteins by recognizing specific NLSs on the latter. We therefore decided

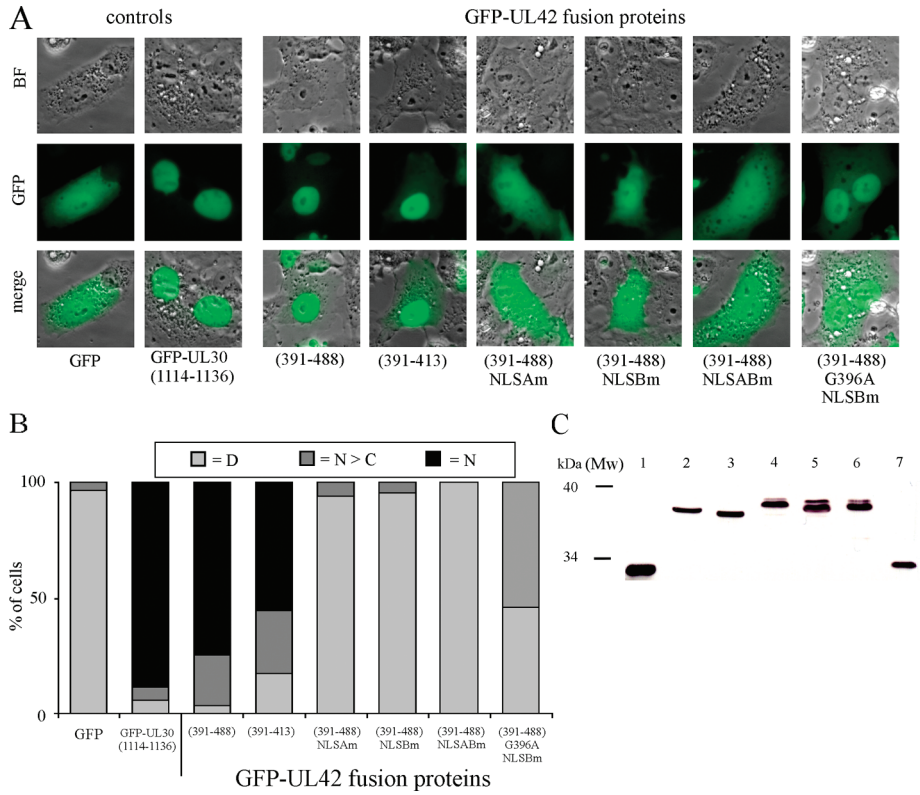

FIGURE 4: UL42 residues 391−413 are sufficient and necessary to target GFP to the nucleus. (A) Fluorescent images of live COS-7 cells 16−24 h after transfection to express the indicated GFP fusion proteins. The bright field (BF) and the green (GFP) channels are shown, and a merged image (merge) is shown in the bottom panels. (B) GFP-expressing cells (n > 100) were scored on the basis of the GFP fusion subcellular localization. N = exclusively nuclear; N > C = more nuclear than cytoplasmic; D = diffuse (see Materials and Methods). (C) COS-7 cells expressing GFP fusion proteins were lysed, separated by PAGE and analyzed by Western blotting as described in the Materials and Methods section, (1) GFP; (2) GFP−UL42(391−488); (3) GFP−UL42(391−488)-NLSAm; (4) GFP−UL42(391−488)-NLSBm; (5) GFP−UL42(391−488)-NLSABm; (6) GFP−UL42(391−488);G396A-NLSBm; (7) GFP−UL42(391−413).

to analyze the UL42 primary sequence for the presence of putative NLSs responsible for its nuclear targeting. Sequence analysis performed using the PSORT software (*45*) revealed the presence of two putative monopartite NLSs: PTTKRGR^{397} (NLSA) and KKPK^{413} (NLSB). Intriguingly the two NLSs, despite matching the consensus for IMPα/β binding, contain residues in position +3 of the NLS core that could impair IMPα binding and are closely located, defining a putative bipartite NLS (NLSbip, PTTKRGRSGGEDARADTALKKPK^{413}) strongly resembling the one we recently identified on HSV-1 UL30 (*20*), which appears to be conserved among other α-herpesviruses, including human HSV-2 (see Figure 2C). To test the role of these sequences in UL42 nuclear import, we expressed several mutant derivatives of UL42 fused to GFP (Figure 2A) in mammalian cells, and analyzed their subcellular localization by live cell imaging. We also analyzed the localization of GFP−UL44(2−433) and GFP−UL44ΔNLS (*16*) as positive and negative controls for nuclear targeting, respectively. As expected, GFP−UL44(2−433) localized to the nucleus of transfected cells, whereas GFP−UL44ΔNLS was retained in the cytoplasm as a consequence of the lack of a functional NLS (Figure 3A). GFP−UL42(2−488) and GFP−UL42(2−413), containing both UL42 putative NLSs, localized strongly to the cell nucleus in almost 100% of analyzed cells, whereas GFP−UL42(2−397), lacking UL42-NLSB, partially localized in the cytoplasm in ca. 75% of analyzed cells, indicating that UL42-NLSA (PTTKRGR^{397}) alone is not sufficient to mediate optimal nuclear targeting of UL42 (see Figure 3A,B). Localization of GFP−UL42(2−390), which lacks both UL42-NLSs, was even more cytoplasmic, being exclusively nuclear only in ca. 10% of transfected cells (Figure 3A,B). These results indicate that UL42 CTD is responsible for active nuclear transport and that UL42-NLSA, despite matching the consensus for a monopartite NLS (*20*), is not fully functional in terms of nuclear import in the absence of NLSB.

UL42 Residues 391−413 Confer Nuclear Accumulation to GFP. To identify the UL42-NLS, defined as the minimal sequence sufficient to confer nuclear targeting to a heterologous protein, we expressed in COS-7 cells several UL42 mutant derivatives fused to GFP and compared their subcellular localization to that of GFP alone and that of GFP−UL30(1114−1136), a fusion protein between GFP and the classical bipartite NLS of HSV-1 DNA polymerase catalytic subunit (*20*). As expected, GFP alone localized with a diffuse pattern in both the nucleus and cytoplasm of transfected cells, while GFP−UL30(1114−1136) accumulated within the cell nucleus (Figure 4A,B). Importantly, GFP−UL42(391−488) and GFP−UL42(391−413) localized to the nucleus of transfected cells. In contrast, GFP−UL42(391−488)-NLSAm, GFP−UL42(391−488)-NLSBm, and GFP−UL42(391−488)-NLSABm, containing point mutations within the basic core of NLSA, NLSB, or both, respectively (see Materials and Methods), failed to accumulate in the nucleus. These results show that both basic stretches present in UL42 CTD are required for NLS function, implying that both UL42-NLSA (PTTKRGR^{397})

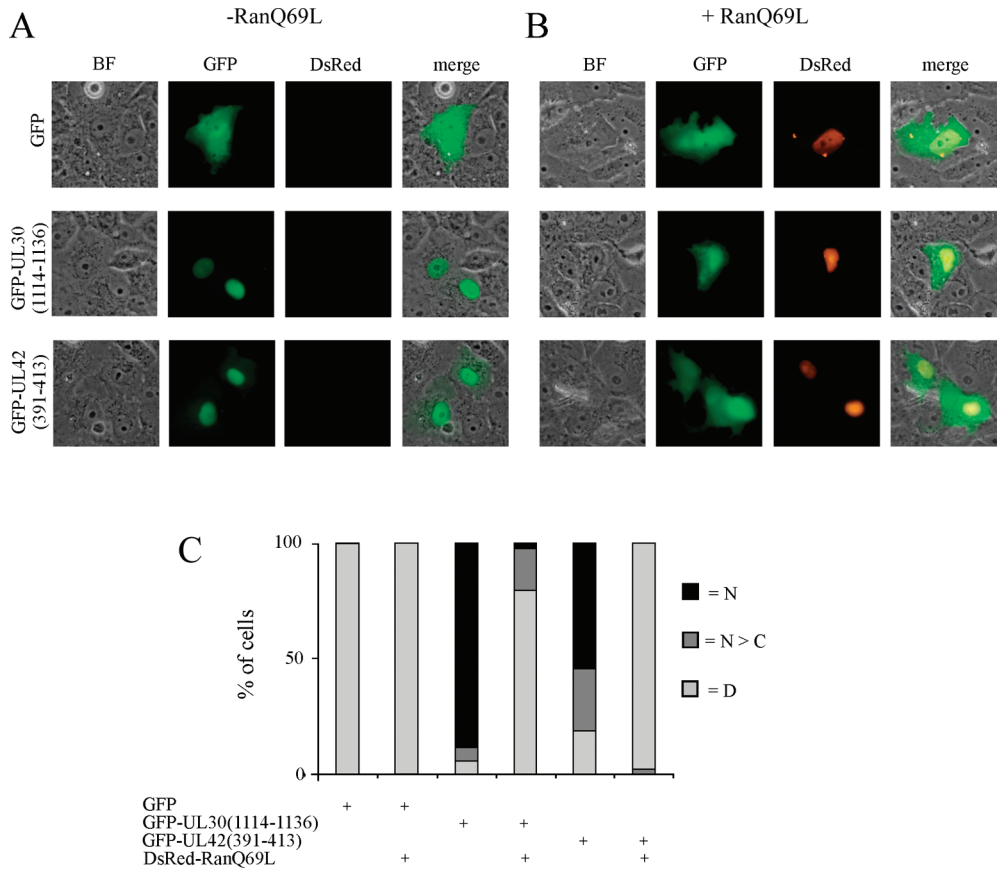

FIGURE 5: UL42-NLSbip mediated nuclear import is inhibited by RanQ69L. Fluorescent images of live COS-7 cells 16−24 h after transfection to express the indicated GFP fusion proteins in the absence (A) or presence (B) of DsRed−RanQ69L. The bright field (BF), green (GFP), and red (DsRed) channels are shown, and a merged image is shown in the right panels. (C) Classification of the degree of nuclear localization of the indicated GFP fusion proteins on the basis of their subcellular localization as shown in panels A and B ($n > 50$). N = exclusively nuclear; N > C = more nuclear than cytoplasmic; D = diffuse (see Materials and Methods).

and UL42-NLSB (KKPK^{413}) are not functional as monopartite NLSs. That the aforementioned mutant derivatives of UL42 are still capable of partially entering the nucleus is likely due to passive diffusion rather than active nuclear transport, since their apparent molecular weight is well below the NPC cutoff for diffusion (Figure 4C).

We have already shown that the presence of a P residue in position +3 of the NLS core is not compatible with nuclear transport as mediated by monopartite NLSs, which explains the lack of functionality of UL42-NLSB as a monopartite NLS (*46*), and we reasoned that the G residue in position +3 of UL42-NLSA could similarly prevent its activity as a monopartite NLS. To test this hypothesis, we analyzed the subcellular localization of GFP−UL42(391−488);G396A-NLSBm, a point mutant derivative carrying a G to A substitution in position +3 within the core of UL42-NLSA, and point mutations within UL42-NLSB (PTTKRaRSGGE-DARADrgLlePK^{413}), when transiently expressed in COS-7 cells. As expected, the G396A substitution in position 3 of UL42-NLSA core partially restored nuclear targeting when coupled to the mutation of NLSB, highlighting the negative effect on nuclear import of a G residue present in position +3 of the NLS core (see Figure 4A,B). This hypothesis is further supported by the evidence that GFP−UL42(391−397), containing only UL42-NLSA (PTTKRGR^{397}) localized with a diffuse pattern within the nucleus and the cytoplasm of Vero cells, whereas GFP−UL42(391−397);G396A accumulated preferentially to the cell nucleus (see Figure S1, Supporting Information).

UL42 Residues 391−413 Represent a Functional Bipartite NLS. Our results suggest that UL42 nuclear import is mediated by a bipartite NLS encompassing residues 391−413. However, because molecules up to 60−90 kDa can passively diffuse into the nucleus through the NPC (*47*), it is possible that accumulation of GFP−UL42(391−413) within the nucleus is due to intranuclear binding after passive diffusion rather than to an active import process. To verify that UL42(391−413) is a functional NLS, we analyzed the localization of GFP−UL42(391−413) in the presence of DsRed−RanQ69L when transiently expressed in COS-7 cells. We also expressed GFP−UL30(1114−1136) and GFP alone as positive and negative controls for nuclear accumulation, respectively. Coexpression with DsRed−RanQ69L did not influence GFP subcellular localization, whereas it prevented nuclear accumulation of GFP−UL30(1114−1136) and GFP−UL42(391−413), indicating that UL42 residues 391−413 represent a functional bipartite NLS (Figure 5).

To confirm this hypothesis, we investigated the energy requirements of GFP−UL42(391−413) nuclear accumulation. We expressed GFP−UL30(1114−1136), GFP−H1E, GFP−UL42(391−413), and GFP alone in COS-7 cells. All proteins except GFP alone localized mainly within the cell nucleus upon normal cell growth conditions (GFP not shown, Figure 6A,B). We then depleted adenosine and guanosine

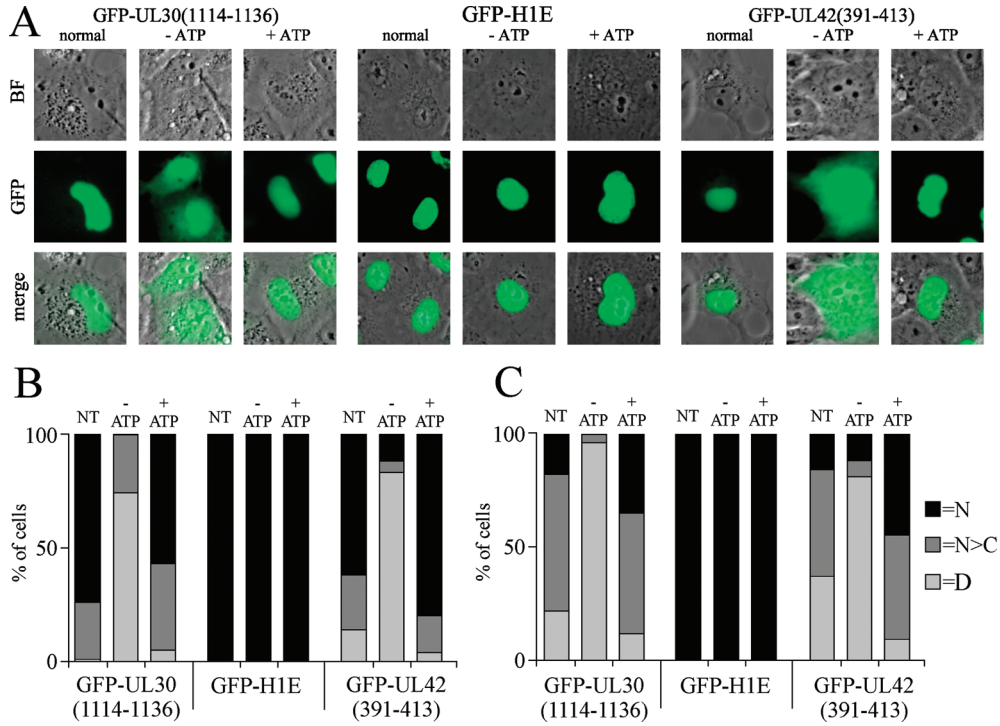

FIGURE 6: UL42 nuclear import is an energy-dependent process. (A) Fluorescent images of live COS-7 cells 16−24 h after transfection to express the indicated GFP fusion proteins. Cells were grown under normal conditions; after imaging (normal; left panels) cells were washed twice in PBS, incubated for 30 min under energy-depletion conditions and imaged (−ATP; middle panels). Within 10 min from restoration of normal growth conditions, cells were imaged again (+ATP; right panels). The bright field (BF) and green (GFP) channels are shown, and a merged image is shown in the bottom panels. (B) GFP-expressing COS-7 cells (n > 100) were scored on the basis of the GFP fusion subcellular localization. N = exclusively nuclear; N > C = more nuclear than cytoplasmic; D = diffuse (see Materials and Methods). (C) GFP-expressing Vero cells (n > 100) were scored on the basis of the GFP fusion subcellular localization. N = exclusively nuclear; N > C = more nuclear than cytoplasmic; D = diffuse (see Materials and Methods).

triphosphates by incubating cells with 2-deoxy-D-glucose and sodium azide (*47*). Within 30 min of such treatment, GFP localization was not affected (not shown), whereas GFP−UL30(1114−1136) equilibrated between the nucleus and the cytoplasm in ca. 75% of the cells analyzed (Figure 6A,B). This result is consistent with our previous finding that UL30(1114−1136) is a functional bipartite NLS, capable of conferring IMPα/β-dependent nuclear targeting properties to heterologous proteins (*20*). On the other hand, energy depletion did not affect nuclear localization of GFP−H1E, consistent with nuclear retention due to DNA binding. Importantly upon energy depletion, GFP−UL42(391−413) localized with a diffuse pattern within the cell nucleus and cytoplasm of ca. 80% of the cells analyzed, demonstrating that its nuclear accumulation under normal growth conditions was due to an active nuclear transport process, similarly to GFP−UL30(1114−1136). The nuclear localization of both GFP−UL30(1114−1136) and GFP−UL42(391−413) was restored within 10 min upon re-establishment of normal growth conditions (see Figure 6A,B), indicating that GFP−UL42 nuclear import is an energy-dependent process. Similar results were obtained in Vero cells (Figure 6C).

UL42-NLSbip Is Required for UL42 Nuclear Targeting in the Absence of Other Viral Proteins. We therefore decided to analyze in detail the contribution of each basic stretch of amino acids forming UL42-NLSbip to the UL42 nuclear import process. We analyzed the subcellular localization of point mutations affecting NLSA and NLSB in the context of full-length UL42 when expressed in Vero cells, which are fully permissive to HSV-1 infection. As expected GFP−UL42(2−488) localized exclusively in the cell nucleus of transfected Vero cells (see Figure 7A,B), whereas point mutant derivatives did not. Inactivation of NLSA had a stronger impact on UL42 nuclear import levels compared with inactivation of NLSB (localizing to the cell nucleus in 35% and 50% of cells, respectively, see Figure 7A,B), whereas combination of mutations within both NLSs abolished nuclear accumulation almost completely (see Figure 7A,B). Similar results were obtained after transfection of COS-7 cells (data not shown), and Western blot analysis revealed that point mutations did not markedly affect protein stability or expression levels (Figure 7C). Our results clearly indicate that both basic stretches of amino acids forming UL42-NLSbip are absolutely required for efficient nuclear targeting of UL42.

UL42 CTD Is Not Required for Targeting to HSV-1 Replication Compartments in Infected Vero Cells. Our data clearly suggest a role for UL42-NLSbip in UL42 nuclear transport. However it has been reported that deletion of UL42 CTD, containing UL42-NLSbip, does not prevent UL42 from localizing to nuclear replication compartments (RCs) during viral infection and only slightly reduces virus titers in cultured cells (*14*). To confirm these findings, we analyzed the subcellular localization of GFP−UL42 fusion proteins in Vero cells transfected and infected with HSV-1 at a MOI of 5. Infected cells were detected with the HD1 gD-specific mAb, recognizing the envelope viral glycoprotein gD (*48*), and cellular chromatin was stained with DAPI in order to facilitate identification of RCs. Infection with HSV-1 rapidly induces chromatin marginalization to the nuclear periphery

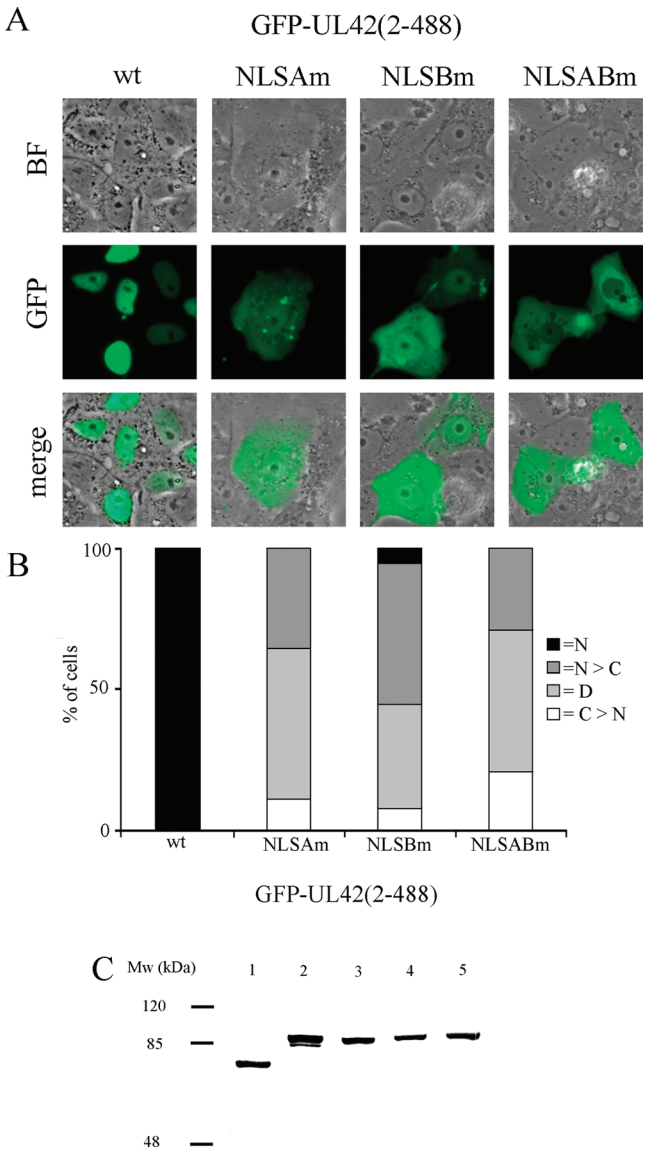

FIGURE 7: UL42 nuclear localization is dependent on a bipartite NLS. (A) Fluorescent images of live Vero cells 16−24 h after transfection to express the indicated GFP fusion proteins. The bright field (BF) and the green (GFP) channels are shown, and a merged image (merge) is shown in the bottom panels. (B) GFP-expressing cells (n > 100) were scored on the basis of the GFP fusion subcellular localization. N = exclusively nuclear; N > C = more nuclear than cytoplasmic; D = diffuse; C > N = more cytoplasmic than nuclear (see Materials and Methods). (C) COS-7 cells expressing GFP fusion proteins were lysed, separated by PAGE, and analyzed by Western blotting as described under the Materials and Methods section, (1) GFP−UL44(2−433); (2) GFP−UL42(2−488); (3) GFP−UL42(2−488)-NLSAm; (4) GFP−UL42(2−488)-NLSBm; (5) GFP−UL42(2−488)-NLSABm.

upon formation of RCs, where viral DNA replication occurs and from which cellular DNA and histones are excluded (*49, 50*). As expected, in mock infected cells GFP−UL42(2−488) exclusively localized to the cell nucleus with a speckled pattern, whereas both GFP−UL42(2−390) and GFP−UL42(2−488)-NLSABm mainly localized to the cytoplasmic compartment (Figure 8A). On the other hand, in HSV-1 infected cells not only GFP−UL42(2−488) but both GFP−UL42(2−390) and GFP−UL42(2−488)NLSABm were recruited to RCs, although some cytoplasmic staining was detectable for the NLS defective mutants (Figure 8B). These results suggest that, in the absence of its functional NLSbip, UL42 could be imported to the nucleus after interaction in the cytoplasm with other viral proteins.

The HSV-1 DNA Polymerase Holoenzyme Can Be Imported to the Nucleus as a Heterodimeric Complex. Since the DNA polymerase holoenzymes from HHV-8 and HCMV can assemble in the cytoplasm before being translocated to the nucleus as multiprotein complexes (*21*), we hypothesized that this could be true for HSV-1 as well. To verify whether HSV DNA polymerase subunits could be translocated to the nucleus as a complex, we coexpressed several GFP−UL30 mutant derivatives with DsRed2−UL42(2−488) and DsRed2−UL42(2−390) and analyzed their subcellular localization. We also expressed DsRed2−UL44(2−433), which is unable to bind to UL30 as a negative control. As expected, both DsRed2−UL42(2−488) and DsRed2−UL44(2−433) localized strongly within the nucleus with a speckled pattern typical of herpetic PAPs, while DsRed2−UL42(2−390) was mainly retained in the cytoplasm of transfected cells as a consequence of the lack of a functional NLS (see Figure 9A,B and ref *22*). That the localization of DsRed2−UL42(2−390) was markedly more cytoplasmic compared with that of GFP−UL42(2−390) is probably due to the tendency of the DsRed2 protein tag to form aggregates when expressed to high levels, thus preventing passive diffusion through the NPC into the nucleus (compare Figures 3A,B and 9A,E). HSV-1 DNA polymerase catalytic subunit GFP−UL30(2−1235) localized within the cell nucleus with a diffuse pattern (Figure 9B), but when coexpressed with DsRed2−UL42(2−488) the two proteins strongly colocalized in nuclear speckles, indicating that the two proteins could efficiently heterodimerize to form the DNA polymerase holoenzyme. No colocalization was observed between GFP−UL30(2−1235) and DsRed2−UL44(2−433). Importantly, coexpression of GFP−UL30(2−1235) with DsRed2−UL42(2−390) resulted in a partial relocalization of the latter to the cell nucleus, with the two proteins colocalizing in nuclear speckles. To further verify the specificity of the observed interactions, we also expressed GFP−UL30(1114−1136), containing UL30 NLSbip but lacking the binding site for UL42 (see also Figure 2B and Table 1), in the absence or in the presence of the aforementioned DsRed2−UL42 fusions. As expected, coexpression with GFP−UL30(1114−1136) had no effect on the subcellular localization DsRed2−UL42(2−390), and no colocalization could be observed between the UL30 and UL42 fusion proteins (Figure 9D,F and Table 1). We also tested the behavior of GFP−UL30(2−1235)-NLS2m, a point mutant derivative containing a point mutation inactivating UL30-NLSbip, but still bearing a noncanonical hydrophobic NLS (NLShyd) located within the binding domain for UL42 (*20, 32*) (see Figure 2B). As previously shown (*20*), when expressed in the absence of other viral proteins GFP−UL30(2−1235)-NLS2m partially entered the nucleus due to the activity of its NLShyd (Figure 9C). Upon coexpression with DsRed2−UL42(2−488), the two proteins strongly colocalized within nuclear speckles, resulting in a marked increase in the nuclear fluorescence of GFP−UL30(2−1235)-NLS2m, suggesting that DsRed2−UL42(2−488) too could piggy back GFP−UL30(2−1235)-NLS2m into the cell nucleus (Figure 9C,F, and Table 1). However, when expressed with DsRed2−UL42(2−390), GFP−UL30(2−1235)-NLS2m was mainly retained in the cytoplasm, presumably due to masking of its NLShyd by

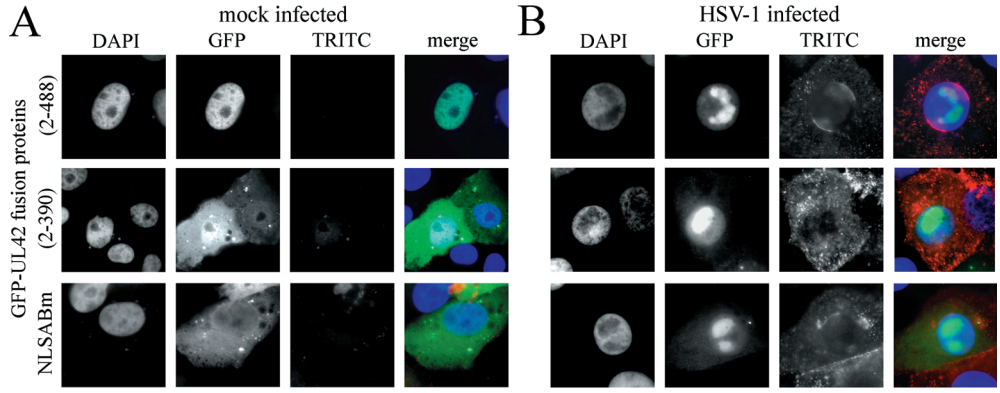

FIGURE 8: UL42 CTD is not required for localization to nuclear replication compartments during viral infection. Images of Vero cells transfected to express the indicated GFP fusion proteins and infected with HSV-1 (5 MOI) 30 h post-transfection. Seven hours postinfection, cells were fixed with methanol/acetone 3:1 and processed by IIFA to detect the late antigen gD. DNA was stained with DAPI. The blue (DAPI), green (GFP), and red (TRITC) channels are shown in gray scale, and a merged CYMK image is shown in the right panels.

UL42 upon interaction with UL30. Taken together, these results suggest that the DNA polymerase holoenzyme can be imported to the nucleus as a complex, so that in the absence of its functional NLS, UL42 can interact with UL30 in the cytoplasm and be translocated to the nucleus via a piggy back mechanism mediated by UL30-NLSbip, which is located outside the UL42-BD on UL30 (*20, 33*).

DISCUSSION

A C-Terminally Located NLS on HSV-1 UL42. This is the first study describing the relevance of the CTD of HSV-1 DNA polymerase processivity factor UL42 to its function, proposing a role for such domain during viral infection. Here we show that UL42 CTD contains a functional bipartite NLS, necessary for efficient nuclear localization, located at residues 391−413. This finding is consistent with the recent identification of functional NLSs at the C-terminus of PAPs from other herpesviruses (*16*−*19*). Our data clearly show that UL42 binds to different IMPα isoforms and localizes exclusively to the cell nucleus when transiently expressed in the absence of other viral proteins, as detected by coimmunoprecipitation assays and fluorescent microscopic analysis of living cells (see Figures 1, 3, 7, 8, and 9). UL42 is transported to the nucleus through a mechanism that is inhibited by RanQ69L, similar to its HCMV (see above) and HHV-7 homologues (*19*). RanQ69L is a dominant negative form of the small GTPase Ran, which lacks the ability to hydrolyze GTP and to bind to NTF2 and is commonly used to inhibit active nuclear import both *in vitro* and *in vivo* (*42, 51, 52*). Since coexpression with RanQ69L resulted in significant relocalization of UL42 to the cytoplasm, we conclude that UL42 is targeted to the cell nucleus via an active process.

Deletion of UL42 CTD resulted in the relocalization of a significant amount of protein to the cytoplasmic compartment, although a considerable amount of protein was still capable of entering the nucleus, and very similar results were obtained by substituting core basic residues within the basic stretches forming UL42-NLSbip (see Figures 3 and 7). The residual nuclear localization observed upon coexpression of GFP−UL42 with RanQ69L or after inactivation of its NLS is likely due to passive diffusion (see Figures 1−4), because molecules with an apparent molecular weight up to 60−90 kDa can still partially diffuse through the NPC (*47*), and the apparent molecular weight of GFP−UL42(2−488) is around 85 kDa (see Figure 7C). This hypothesis is also supported by the evidence that the oligomer forming molecule DsRed2−UL42(2−390) was more cytoplasmic than its GFP-tagged counterpart (see Figure 9A).

Nuclear Import of HSV-1 DNA Polymerase Holoenzyme. Thus, even in the absence of active nuclear import, a fraction of UL42 can enter into the nucleus by passive diffusion. Moreover, it seems likely that the assembly of the HSV-1 DNA polymerase holoenzyme occurs in the cytoplasm before transport into the nucleus, as suggested by our cotransfection experiments (see Figure 9). A mutant of UL42 lacking its functional NLSbip can be retargeted to the nucleus by coexpression with GFP−UL30(2−1235) in the absence of other viral proteins, further supporting our hypothesis that UL30 can piggy-back the UL42 NLS mutant into the cell nucleus (see Figure 9B). Similarly, strong nuclear accumulation of GFP−UL30(2−1235)-NLS2m, a UL30 mutant derivative impaired in nuclear targeting carrying a point mutation inactivating its NLSbip, could be observed upon coexpression with DsRed2−UL42(2−488), indicating that either component of the holoenzyme can complement for mutations inactivating the NLS function on the other subunint. Taken together, these results may explain why a mutant virus bearing only the 338 N-terminal amino acids of UL42, retaining all its known biochemical properties *in vitro* but lacking a functional NLS, is only partially impaired in viral replication, yielding viral titers reduced ca. 3-fold compared with wt virus in Vero cells (*14*). Our results also provide experimental evidence to understand why deletion or mutation of UL42-NLSbips does not prevent UL42 from correctly localizing to viral RCs within the cell nucleus during viral infection (see Figure 8B). Thus our results clearly show that HSV-1 evolved multiple NLSs on its DNA polymerase holoenzyme to maximize nuclear import possibilities. Importantly, mutation of both UL42-NLSbip and UL30-NLSbip results in retention of the DNA polymerase holoenzyme in the cytoplasm (see Figure 9D,F, and Table 1), strongly suggesting that it could be possible to prevent HSV-1 DNA polymerase nuclear targeting by blocking the functionality of both UL30- and UL42-NLSbip.

Why Did HCMV Evolve a Monopartite NLS and HSV-1 Bipartite NLSs on Their DNA Polymerase Subunits? As mentioned earlier, NLSs are similarly located within HCMV

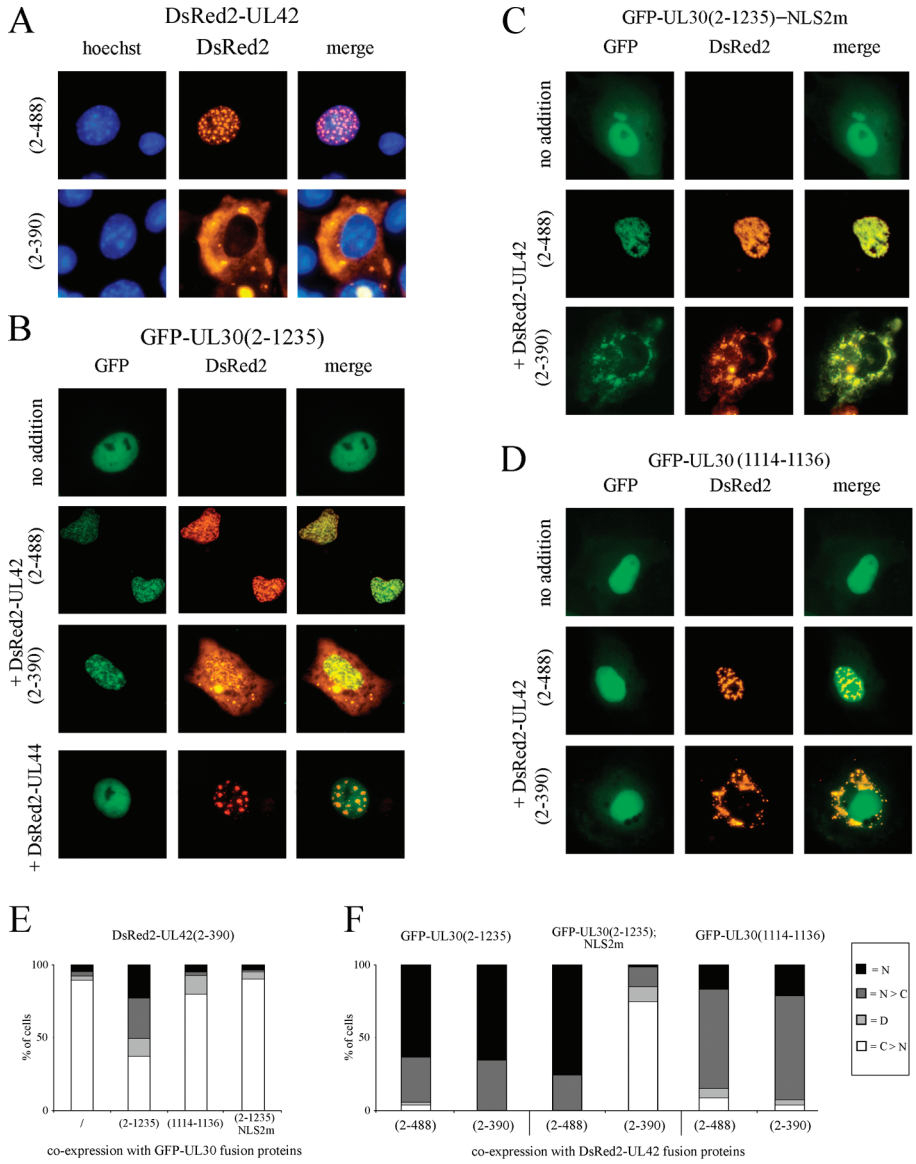

FIGURE 9: HSV-1 DNA polymerase holoenzyme can be translocated to the nucleus as a complex. (A) Images of COS-7 cells transfected to express the indicated DsRed2 fusion proteins and incubated with Hoechst 33342 to visualize DNA. The blue (Hoechst) and red (DsRed2) channels are shown, and a merged image is shown in the right panels. (B−D) Images of COS-7 cells transfected to express the indicated GFP fusion proteins in the absence (no addition) or in the presence of the indicated DsRed2 fusion proteins. The green (GFP) and red (DsRed2) channels are shown, and a merged image (merge) is shown in the right panels. (E) DsRed2−UL42(2−390) expressing cells (n > 100) were scored on the basis of its subcellular localization in the absence (no addition) or in the presence of coexpression with the indicated GFP−UL30 fusion proteins. N = exclusively nuclear; N > C = more nuclear than cytoplasmic; D = diffuse, C > N = more cytoplasmic than nuclear (see Materials and Methods). (F) GFP-expressing cells (n > 100) were scored on the basis of the GFP fusion subcellular localization when expressed in the presence of the indicated DsRed2 fusion protein. N = exclusively nuclear; N > C = more nuclear than cytoplasmic; D = diffuse; C > N = more cytoplasmic than nuclear (see Materials and Methods).

Table 1: Summary of the Effect of Expression of DsRed2−UL42 Fusion Proteins on the Subcellular Localization of GFP−UL30 Fusion Proteins[a]

	presence of functional domains			subcellular localization of GFP−UL30 fusion protein		
GFP−UL30 fusion protein	NLSbip	UL42-BD	NLShyd	no addition	+UL42(2−433)	+UL42(2−390)
GFP−UL30(2−1235)	+	+	+	N	N; Nsp	N; Nsp
GFP−UL30(2−1235)-NLS2m	−	+	+	N > C	N; Nsp	C > N
GFP−UL30(1114−1136)	+	−	−	N > C	N > C	N > C

[a] NLSbip, UL30 bipartite NLS (residues 1114−1136); UL42-BD, UL30 binding domain for UL42 (residues 1209−1235); NLShyd, UL30 hydrophobic NLS (residues 1224−1229); N, exclusively nuclear fluorescence; N > C, significant amount of fluorescence present in the cytoplasm; C > N, mainly cytoplasmic fluorescence; Nsp, colocalizing with DsRed2−UL42 fusions in nuclear speckles.

and HSV-1 DNA polymerase subunits. Both processivity factors possess a C-terminally located NLS, whereas both catalytic subunits possess two functional NLSs, one located within the binding site for their PAP and another located outside such domain (*16, 20, 21, 32*). While it is easy to imagine that the presence of two NLSs on the catalytic subunit is required to maximize the nuclear import possibilities for both the catalytic subunits on their own and as complexed with their processivity factors, it is not clear why HSV-1 evolved bipartite NLSs, whereas HCMV evolved

monopartite NLSs. An explanation for that could lie in the evidence that HSV-1 UL42 and HCMV ppUL44 appear to have different IMP binding capabilities: while ppUL44 binds efficiently only to IMPα6 (and to a lesser extent to IMPα2), belonging to the α-S subtype, UL42 also efficiently bound to the α-Q member IMPα4 (see Figure 1C). Since different IMPα family members have particular cargo specificity and exhibit unique temporal and spatial tissue-specific expression (*26, 27*) and HSV-1 and HCMV possess different cellular tropisms, with HSV-1 being strongly neurotropic (*54*), it is tempting to speculate that HSV-1 evolved bipartite NLSs to ensure optimal nuclear targeting in specific tissues. Further work is required to assess this hypothesis.

A New Consensus for Monopartite NLSs. UL42-NLSbip encompasses two basic stretches of amino acids (NLSA, PTTKRGR^{397}; NLSB, KKPK^{413}), both of which are required for NLS function (see Figures 5−7). Intriguingly both stretches match the consensus for putative monopartite NLSs, (K)-(K/R)-(X)-(K/R) (*30*), but possess a G and a P residue in position +3 of the NLS core, respectively. We have recently shown that a P residue in position +3 of the NLS core is not compatible with monopartite NLS activity (*20*), and here we suggest that a G residue in position +3 of the NLS core could similarly be not compatible with monopartite NLS function (see Figure 4). Consistent with our hypothesis, we showed that the sequence PTTKRaR^{397} but not PTTKRGR^{397} is capable of targeting GFP to the cell nucleus (see Figure 4 and Figure S1, Supporting Information). Our results have thus relevance for the identification of classical monopartite NLSs and further support the redefinition of the consensus motif for monopartite NLSs to (K)-(K/R)-(X′)-(K/R), where X′ is any amino acid apart from P or G. The extreme rigidity/flexibility conferred by such residues, respectively, can be overcome by the presence of additional basic residues surrounding the NLS as in the case of the mouse polycomb protein, M33 (*53*), or by the presence of an additional stretch of basic residues located within 10−12 amino acids, thus forming a bipartite NLS as in the case of HSV-1 UL30 (*20*). Consistent with this hypothesis, putative bipartite NLSs resembling that identified here are located within UL42 homologues from several α-herpesviruses, including human HSV-2 and cercopithecine and suid HSV-1 (see Figure 2C).

CONCLUSIONS AND PERSPECTIVES

The data presented here allow us to clearly define UL42 nuclear import as an energy-dependent, IMPα/*β*-mediated process, which is impaired by RanQ69L and depends on a C-terminally located bipartite NLS. Our results should prove determinant for the understanding of the controversial role played by UL42 CTD during viral infection, explaining why a mutant virus lacking the 150 C-terminal amino acids of UL42 yielded infectious titers reduced almost 3 times compared with a virus encoding full-length UL42, although all known biochemical properties of UL42 reside in its N-terminal domain. These findings could constitute the basis for the development of new anti-HSV-1 therapeutics based on the inhibition of the DNA polymerase holoenzyme nuclear import. Furthermore, the definition of a new consensus for a monopartite NLS should help the identification of novel functional NLSs.

ACKNOWLEDGMENT

We thank Gabriella Campadelli-Fiume (University of Bologna) for mouse mAb HD1 directed against HSV-1 structural protein gD, and Charles Hwang (State University of New York Upstate Medical University), Michael Green (University of Massachusetts), Gabi Gerlitz (NIH), Yoichi Miyamoto (Monash University), and Emanuele Panza (University of Bologna) for providing plasmids.

SUPPORTING INFORMATION AVAILABLE

Figure demonstrating that the presence of a G residue at position +3 of UL42-NLSA core impairs its functionality. This material is available free of charge via the Internet at http://pubs.acs.org.

REFERENCES

1. Roizman, B., and Whitley, R. J. (2001) The nine ages of herpes simplex virus. *Herpes 8*, 23–27.
2. Wu, C. A., Nelson, N. J., McGeoch, D. J., and Challberg, M. D. (1988) Identification of herpes simplex virus type 1 genes required for origin-dependent DNA synthesis. *J. Virol. 62*, 435–443.
3. Gottlieb, J., Marcy, A. I., Coen, D. M., and Challberg, M. D. (1990) The herpes simplex virus type 1 UL42 gene product: A subunit of DNA polymerase that functions to increase processivity. *J. Virol. 64*, 5976–5987.
4. Chaudhuri, M., and Parris, D. S. (2002) Evidence against a simple tethering model for enhancement of herpes simplex virus DNA polymerase processivity by accessory protein UL42. *J. Virol. 76*, 10270–10281.
5. Jiang, C., Hwang, Y. T., Wang, G., Randell, J. C., Coen, D. M., and Hwang, C. B. (2007) Herpes simplex virus mutants with multiple substitutions affecting DNA binding of UL42 are impaired for viral replication and DNA synthesis. *J. Virol. 81*, 12077–12079.
6. Jiang, C., Hwang, Y. T., Randell, J. C., Coen, D. M., and Hwang, C. B. (2007) Mutations that decrease DNA binding of the processivity factor of the herpes simplex virus DNA polymerase reduce viral yield, alter the kinetics of viral DNA replication, and decrease the fidelity of DNA replication. *J. Virol. 81*, 3495–3502.
7. Komazin-Meredith, G., Mirchev, R., Golan, D. E., van Oijen, A. M., and Coen, D. M. (2008) Hopping of a processivity factor on DNA revealed by single-molecule assays of diffusion. *Proc. Natl. Acad. Sci. U.S.A. 105*, 10721–10726.
8. Komazin-Meredith, G., Santos, W. L., Filman, D. J., Hogle, J. M., Verdine, G. L., and Coen, D. M. (2008) The positively charged surface of herpes simplex virus UL42 mediates DNA binding. *J. Biol. Chem. 283*, 6154–6161.
9. Marsden, H. S., Campbell, M. E., Haarr, L., Frame, M. C., Parris, D. S., Murphy, M., Hope, R. G., Muller, M. T., and Preston, C. M. (1987) The 65,000-Mr DNA-binding and virion trans-inducing proteins of herpes simplex virus type 1. *J. Virol. 61*, 2428–2437.
10. Pilger, B. D., Cui, C., and Coen, D. M. (2004) Identification of a small molecule that inhibits herpes simplex virus DNA Polymerase subunit interactions and viral replication. *Chem. Biol. 11*, 647–654.
11. Hamatake, R. K., Bifano, M., Tenney, D. J., Hurlburt, W. W., and Cordingley, M. G. (1993) The herpes simplex virus type 1 DNA polymerase accessory protein, UL42, contains a functional protease-resistant domain. *J. Gen. Virol. 74* (10), 2181–2189.
12. Monahan, S. J., Barlam, T. F., Crumpacker, C. S., and Parris, D. S. (1993) Two regions of the herpes simplex virus type 1 UL42 protein are required for its functional interaction with the viral DNA polymerase. *J. Virol. 67*, 5922–5931.
13. Tenney, D. J., Hurlburt, W. W., Bifano, M., Stevens, J. T., Micheletti, P. A., Hamatake, R. K., and Cordingley, M. G. (1993) Deletions of the carboxy terminus of herpes simplex virus type 1 UL42 define a conserved amino-terminal functional domain. *J. Virol. 67*, 1959–1966.
14. Gao, M., DiTusa, S. F., and Cordingley, M. G. (1993) The C-terminal third of UL42, a HSV-1 DNA replication protein, is dispensable for viral growth. *Virology 194*, 647–653.
15. Goodrich, L. D., Rixon, F. J., and Parris, D. S. (1989) Kinetics of expression of the gene encoding the 65-kilodalton DNA-binding protein of herpes simplex virus type 1. *J. Virol. 63*, 137–147.

16. Alvisi, G., Jans, D. A., Guo, J., Pinna, L. A., and Ripalti, A. (2005) A protein kinase CK2 site flanking the nuclear targeting signal enhances nuclear transport of human cytomegalovirus ppUL44. *Traffic 6*, 1002–1013.
17. Chen, Y., Ciustea, M., and Ricciardi, R. P. (2005) Processivity factor of KSHV contains a nuclear localization signal and binding domains for transporting viral DNA polymerase into the nucleus. *Virology 340*, 183–191.
18. Loh, L. C., Keeler, V. D., and Shanley, J. D. (1999) Sequence requirements for the nuclear localization of the murine cytomegalovirus M44 gene product pp50. *Virology 259*, 43–59.
19. Takeda, K., Haque, M., Nagoshi, E., Takemoto, M., Shimamoto, T., Yoneda, Y., and Yamanishi, K. (2000) Characterization of human herpesvirus 7 U27 gene product and identification of its nuclear localization signal. *Virology 272*, 394–401.
20. Alvisi, G., Musiani, D., Jans, D. A., and Ripalti, A. (2007) An importin alpha/beta-recognized bipartite nuclear localization signal mediates targeting of the human herpes simplex virus type 1 DNA polymerase catalytic subunit pUL30 to the nucleus. *Biochemistry 46*, 9155–9163.
21. Alvisi, G., Ripalti, A., Ngankeu, A., Giannandrea, M., Caraffi, S. G., Dias, M. M., and Jans, D. A. (2006) Human cytomegalovirus DNA polymerase catalytic subunit pUL54 possesses independently acting nuclear localization and ppUL44 binding motifs. *Traffic 7*, 1322–1332.
22. Stewart, M. (2007) Molecular mechanism of the nuclear protein import cycle. *Nat. Rev. Mol. Cell Biol. 8*, 195–208.
23. Cingolani, G., Petosa, C., Weis, K., and Muller, C. W. (1999) Structure of importin-beta bound to the IBB domain of importin-alpha. *Nature 399*, 221–229.
24. Lee, S. J., Matsuura, Y., Liu, S. M., and Stewart, M. (2005) Structural basis for nuclear import complex dissociation by RanGTP. *Nature 435*, 693–696.
25. Gorlich, D., Pante, N., Kutay, U., Aebi, U., and Bischoff, F. R. (1996) Identification of different roles for RanGDP and RanGTP in nuclear protein import. *EMBO J. 15*, 5584–5594.
26. Hogarth, C. A., Calanni, S., Jans, D. A., and Loveland, K. L. (2006) Importin alpha mRNAs have distinct expression profiles during spermatogenesis. *Dev. Dyn. 235*, 253–262.
27. Jans, D. A., Xiao, C. Y., and Lam, M. H. (2000) Nuclear targeting signal recognition: a key control point in nuclear transport? *Bioessays 22*, 532–544.
28. Lange, A., Mills, R. E., Lange, C. J., Stewart, M., Devine, S. E., and Corbett, A. H. (2007) Classical nuclear localization signals: Definition, function, and interaction with importin alpha. *J. Biol. Chem. 282*, 5101–5105.
29. Conti, E., Uy, M., Leighton, L., Blobel, G., and Kuriyan, J. (1998) Crystallographic analysis of the recognition of a nuclear localization signal by the nuclear import factor karyopherin alpha. *Cell 94*, 193–204.
30. Hodel, M. R., Corbett, A. H., and Hodel, A. E. (2001) Dissection of a nuclear localization signal. *J. Biol. Chem. 276*, 1317–1325.
31. Prichard, M. N., Lawlor, H., Duke, G. M., Mo, C., Wang, Z., Dixon, M., Kemble, G., and Kern, E. R. (2005) Human cytomegalovirus uracil DNA glycosylase associates with ppUL44 and accelerates the accumulation of viral DNA. *Virol. J. 2*, 55.
32. Loregian, A., Piaia, E., Cancellotti, E., Papini, E., Marsden, H. S., and Palu, G. (2000) The catalytic subunit of herpes simplex virus type 1 DNA polymerase contains a nuclear localization signal in the UL42-binding region. *Virology 273*, 139–148.
33. Marsden, H. S., Murphy, M., McVey, G. L., MacEachran, K. A., Owsianka, A. M., and Stow, N. D. (1994) Role of the carboxy terminus of herpes simplex virus type 1 DNA polymerase in its interaction with UL42. *J. Gen. Virol. 75* (11), 3127–3135.
34. Poon, I. K., Oro, C., Dias, M. M., Zhang, J., and Jans, D. A. (2005) Apoptin nuclear accumulation is modulated by a CRM1-recognized nuclear export signal that is active in normal but not in tumor cells. *Cancer Res. 65*, 7059–7064.
35. Hubner, S., Eam, J. E., Wagstaff, K. M., and Jans, D. A. (2006) Quantitative analysis of localization and nuclear aggregate formation induced by GFP-lamin A mutant proteins in living HeLa cells. *J. Cell. Biochem. 98*, 810–826.
36. Panza, E., Marini, M., Pecci, A., Giacopelli, F., Bozzi, V., Seri, M., Balduini, C., and Ravazzolo, R. Transfection of the mutant MYH9 cDNA reproduces the most typical cellular phenotype of MYH9-related disease in different cell lines, *PathoGenetics*, in press.
37. Miyamoto, Y., Hieda, M., Harreman, M. T., Fukumoto, M., Saiwaki, T., Hodel, A. E., Corbett, A. H., and Yoneda, Y. (2002) Importin alpha can migrate into the nucleus in an importin beta- and Ran-independent manner. *EMBO J. 21*, 5833–5842.
38. Alvisi, G., Jans, D. A., and Ripalti, A. (2006) Human cytomegalovirus (HCMV) DNA polymerase processivity factor ppUL44 dimerizes in the cytosol before translocation to the nucleus. *Biochemistry 45*, 6866–6872.
39. Heilman, D. W., Teodoro, J. G., and Green, M. R. (2006) Apoptin nucleocytoplasmic shuttling is required for cell type-specific localization, apoptosis, and recruitment of the anaphase-promoting complex/cyclosome to PML bodies. *J. Virol. 80*, 7535–7545.
40. Gerlitz, G., Livnat, I., Ziv, C., Yarden, O., Bustin, M., and Reiner, O. (2007) Migration cues induce chromatin alterations. *Traffic 8*, 1521–1529.
41. Bauerle, M., Doenecke, D., and Albig, W. (2002) The requirement of H1 histones for a heterodimeric nuclear import receptor. *J. Biol. Chem. 277*, 32480–32489.
42. Stewart, M., Kent, H. M., and McCoy, A. J. (1998) The structure of the Q69L mutant of GDP-Ran shows a major conformational change in the switch II loop that accounts for its failure to bind nuclear transport factor 2 (NTF2). *J. Mol. Biol. 284*, 1517–1527.
43. Fontes, M. R., Teh, T., Toth, G., John, A., Pavo, I., Jans, D. A., and Kobe, B. (2003) Role of flanking sequences and phosphorylation in the recognition of the simian-virus-40 large T-antigen nuclear localization sequences by importin-alpha. *Biochem. J. 375*, 339–349.
44. Kobe, B. (1999) Autoinhibition by an internal nuclear localization signal revealed by the crystal structure of mammalian importin alpha. *Nat. Struct. Biol. 6*, 388–397.
45. Nakai, K., and Horton, P. (1999) PSORT: A program for detecting sorting signals in proteins and predicting their subcellular localization. *Trends Biochem. Sci. 24*, 34–36.
46. Advani, S. J., Weichselbaum, R. R., and Roizman, B. (2003) Herpes simplex virus 1 activates cdc2 to recruit topoisomerase II alpha for post-DNA synthesis expression of late genes. *Proc. Natl. Acad. Sci. U.S.A. 100*, 4825–4830.
47. Cardarelli, F., Serresi, M., Bizzarri, R., Giacca, M., and Beltram, F. (2007) In vivo study of HIV-1 Tat arginine-rich motif unveils its transport properties. *Mol. Ther. 15*, 1313–22.
48. Dix, R. D., Pereira, L., and Baringer, J. R. (1981) Use of monoclonal antibody directed against herpes simplex virus glycoproteins to protect mice against acute virus-induced neurological disease. *Infect. Immun. 34*, 192–199.
49. Dupuy-Coin, A. M., Arnoult, J., and Bouteille, M. (1978) Quantitative correlation of morphological alterations of the nucleus with functional events during in vitro infection of glial cells with herpes simplex hominis (HSV 2). *J. Ultrastruct. Res. 65*, 60–72.
50. Monier, K., Armas, J. C., Etteldorf, S., Ghazal, P., and Sullivan, K. F. (2000) Annexation of the interchromosomal space during viral infection. *Nat. Cell Biol. 2*, 661–665.
51. Avis, J. M., and Clarke, P. R. (1996) Ran, a GTPase involved in nuclear processes: its regulators and effectors. *J. Cell Sci. 109* (10), 2423–2427.
52. Bischoff, F. R., Klebe, C., Kretschmer, J., Wittinghofer, A., and Ponstingl, H. (1994) RanGAP1 induces GTPase activity of nuclear Ras-related Ran. *Proc. Natl. Acad. Sci. U.S.A. 91*, 2587–2591.
53. Hirose, S., Komoike, Y., and Higashinakagawa, T. (2006) Identification of a nuclear localization signal in mouse polycomb protein, M33. *Zool. Sci. 23*, 785–791.
54. Bello-Morales, R., Fedetz, M., Alcina, A., Tabares, E., and Lopez-Guerrero, J. A. (2005) High susceptibility of a human oligodendroglial cell line to herpes simplex type 1 infection. *J. Neurovirol. 11*, 190–198.

BI800869Y